

Magnetic fingerprints of fractal spectra and the duality of Hofstadter models

O Gat and J E Avron

Department of Physics, Technion, 32000, Haifa, Israel

E-mail: omri@physics.technion.ac.il and

avron@physics.technion.ac.il

New Journal of Physics 5 (2003) 44.1–44.8 (<http://www.njp.org/>)

Received 5 February 2003

Published 12 May 2003

Abstract. We study the de Haas–van Alphen oscillations in the magnetization of the Hofstadter model. Near a split band the magnetization is a rapidly oscillating function of the Fermi energy with lip-shaped envelopes. For generic magnetic fields this structure appears on all scales and provides a thermodynamic fingerprint of the fractal properties of the model. The analysis applies equally well to the two dual interpretations of the Hofstadter model and the nature of the duality transformation is elucidated.

The Hofstadter model [1] describes non-interacting (spinless) electrons moving in the plane under the combined action of a magnetic field and a periodic potential. The model is a paradigm for quantum systems with singular continuous spectra [2, 3], Chern numbers in the integer quantum Hall effect [4], fractal quantum phase diagrams [5], quantum integrable models [6] and non-commutative geometry [7]. It has been realized experimentally in [8] and measurements of the Hall conductance phase diagram are in good agreement with the theoretical predictions of [4].

Previous studies of the thermodynamics of the Hofstadter model have focused on the minima of the ground state energy [9]. Our aim is to examine the possibility that the de Haas–van Alphen oscillations, which are a basic tool in the study of the geometry of the Fermi surfaces of metals [10], also provide a tool for studying its non-commutative analogue. We show that when the magnetic flux per unit cell is close to a rational multiple of the flux quantum, the magnetization oscillates as a function of the chemical potential in the vicinity of the bands of the rational flux, as in the de Haas–van Alphen effect. As the deviation from rational flux becomes smaller, the frequency of the oscillations increases, so that in the limit of the deviation tending to zero the oscillations fill an area bounded by a limiting envelope. The envelopes have the following universal features: they are smooth functions of the chemical potential except for logarithmic pinching at a single point, associated with a logarithmic divergence of the density of states, and they are pinched linearly at the edges of the bands. These properties give the envelopes distinctive lip-like shapes.

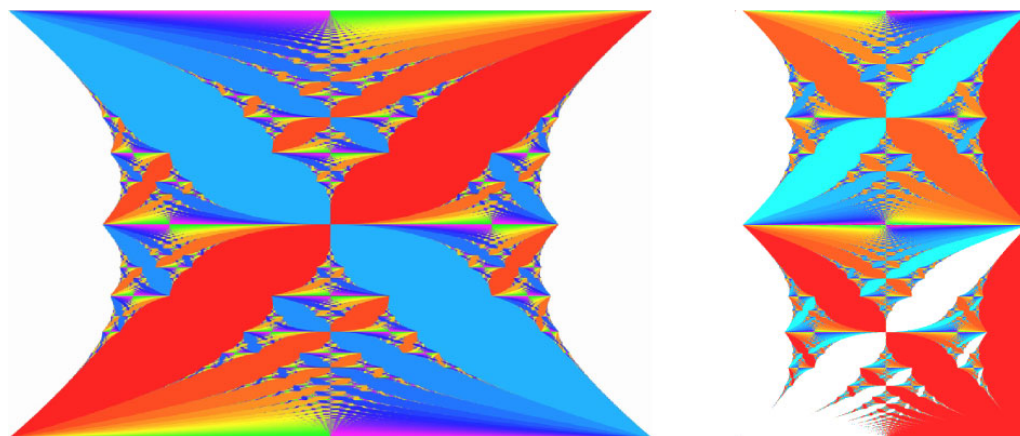


Figure 1. The quantum phase diagrams of a split Bloch band (left) and split Landau level (right). The horizontal axis is the chemical potential and the vertical axis is $0 \leq \varphi \leq 1$ on the left and $0 \leq \varphi^{-1} \leq 2$ on the right. The colours represent the quantized Hall conductances. The scheme is such that cold colours correspond to negative integers and warm colours positive integers. Zero is white. The red on the right-hand side of the right diagram corresponds to unit Hall conductance of a full Landau band.

It follows from these results that, at magnetic flux ratios which are irrational numbers well approximated by infinitely many rational numbers, magnetic oscillations bounded by lip-shaped envelopes occur on all energy scales. In this sense, the magnetic oscillations provide a fingerprint of the fractal spectra of the model.

A second issue of the Hofstadter model that we discuss is duality. The Hofstadter model approximates the Schrödinger equation in two dual limits: when the magnetic field is a weak perturbation of a Bloch band and remarkably also in the dual limit when the magnetic field is so strong that the periodic potential is a perturbation of the lowest Landau level. As we shall see, the thermodynamic properties of the dual limits are related by an interesting duality transformation of the thermodynamic potential, equation (3) below. We examine the consequences of the duality for the magnetization and the Hall conductance in some detail.

The spectral analysis of the Hofstadter model reduces to studying a family of one dimensional problems parameterized by a conserved quasi-momentum ξ . For the sake of concreteness and simplicity we shall consider the case where the periodic potential has square symmetry. In this case the corresponding Hamiltonian is:

$$(H(\varphi, \xi)\psi)(j) = \psi(j-1) + \psi(j+1) + 2 \cos(2\pi\varphi j + \xi) \psi(j). \quad (1)$$

It is known that H describes the splitting of a Bloch band by a weak transverse magnetic field, and also the splitting of a Landau level by a weak periodic potential. φ and φ^{-1} are the values of flux through a unit cell, measured in units of quantum flux $\Phi_0 = hc/e$, in the split Bloch and split Landau cases, respectively. Note that φ is a dimensionless quantity.

Although $H(\varphi, \xi)$ depends analytically on φ its spectral properties are sensitive to the flux; when φ is a rational number the spectrum is a finite collection of energy bands, while for (almost all) irrational fluxes it is a Cantor set of zero Lebesgue measure [3].

Let $\Omega_b(T, \mu, \varphi)$ be the thermodynamic potential per unit cell of a split Bloch band. By

gauge invariance, time-reversal and electron–hole symmetry, Ω_b satisfies

$$\begin{aligned}\Omega_b(T, \mu, \varphi) &= \Omega_b(T, \mu, -\varphi) \\ &= \Omega_b(T, \mu, \varphi + 1) = \mu + \Omega_b(T, -\mu, \varphi).\end{aligned}\quad (2)$$

It follows that the thermodynamic properties for all φ and μ are determined by those for $0 \leq \varphi \leq 1/2$, $\mu < 0$. $\mu = 0$ corresponds to the half-filling point of electron–hole symmetry. The phase diagram of the split Bloch band is displayed on the left-hand side of figure 1. The phases are labelled by the values of the Hall conductance, whose relation to Ω is given in equation (4) below. The phase diagram displays the symmetry properties shown in equation (2). The phase diagram is periodic in φ , see equation (2); a single period is given in figure 1.

It is straightforward to get from the thermodynamics of the split Bloch band to that of the split Landau level by observing that the energy spectra of the two models are the same. The difference is that the number of states per unit area in a split Bloch band is a constant independent of the magnetic field, whereas the number of states per unit area of a Landau level is proportional to the magnetic field. Therefore the thermodynamic potentials of a split Landau level, Ω_l , and split Bloch band are related by

$$\Omega_l(T, \mu, \varphi) = \varphi \Omega_b(T, \mu, \varphi^{-1}).\quad (3)$$

This is a duality transformation: it is symmetric under the interchange $b \longleftrightarrow l$. It implies that the thermodynamics of the split Bloch band determine the thermodynamics of a split Landau level and vice versa. It follows from equation (3) that Ω_l is not periodic, although Ω_b is, simply because of the factor φ on the right. A part of the phase diagram of the split Landau level is shown on the right-hand side of figure 1, and it is evidently aperiodic.

To derive the relation between the magnetization and Hall conductances of the two models recall that the filling fraction, ρ , the magnetization per unit area, m , and Hall conductance [11], σ , are given by

$$\rho = \left(\frac{\partial \Omega}{\partial \mu}\right)_\varphi, \quad m = -\frac{1}{\Phi_0} \left(\frac{\partial \Omega}{\partial \varphi}\right)_\mu, \quad \sigma = \frac{e^2}{h} \left(\frac{\partial \rho}{\partial \varphi}\right)_\mu.\quad (4)$$

The magnetization and the Hall conductances of the two models are therefore related by:

$$\begin{aligned}m_l(\mu, T, \varphi^{-1}) &= \frac{1}{\Phi_0} \Omega_b(\mu, T, \varphi) - \varphi m_b(\mu, T, \varphi), \\ \sigma_l(\mu, T, \varphi^{-1}) &= \frac{e^2}{h} \rho_b(\mu, T, \varphi) - \varphi \sigma_b(\mu, T, \varphi).\end{aligned}\quad (5)$$

The duality relation of the Hall conductances is a generalization of a relation that follows from the Diophantine equation in [4].

The magnetization is related to the Hall conductance by the Maxwell relation

$$-\left(\frac{\partial m}{\partial \mu}\right)_\varphi = \frac{1}{\Phi_0} \left(\frac{\partial \rho}{\partial \varphi}\right)_\mu = \frac{1}{ec} \sigma.\quad (6)$$

It follows that, whenever the Hall conductance is quantized, the magnetization has a quantized slope that is an integer multiple of $1/\Phi_0$. In the Hofstadter model σ_b and σ_l are quantized in the gaps [4, 12]. It follows that the magnetization has quantized (and therefore also constant) slopes in the gaps.

We now turn to a more detailed study of the magnetization in the gaps at $T = 0$, starting with m_b . For a fixed rational φ this is a finite collection of lines. From equations (2) and (4) it follows that m_b is a symmetric function of μ .

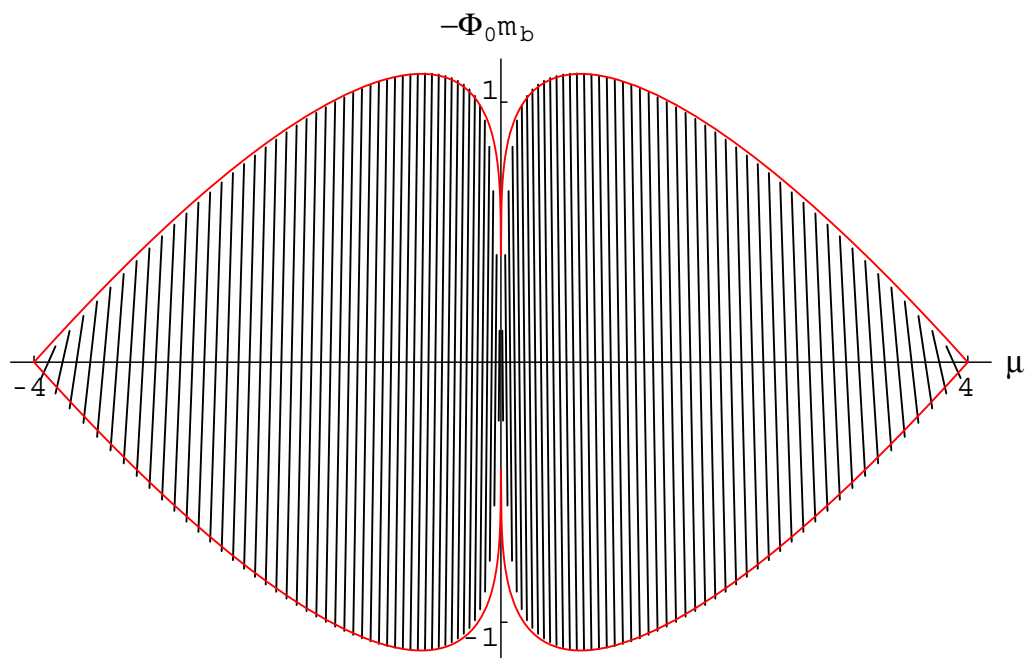


Figure 2. The graph of the magnetization m_b of a split Bloch band with $\varphi = 1/101$. When φ tends to zero the magnetization has a limiting envelope denoted by $L_b(\mu, 0)$.

When $\varphi = p/q$, with p and q relatively prime, the magnetization can be computed numerically. In this case the potential in equation (1) is periodic with period q and the spectral analysis of $H(\varphi, \xi)$ further reduces to the study of $q \times q$ matrices $\mathbf{H}(\varphi, \xi, \eta)$ labelled by a second Bloch (quasi) momentum η . The magnetization $m_b(\mu, \varphi)$ in the gap of a split Bloch band can be shown to be given by

$$-\frac{q}{2\pi\Phi_0} \sum_{\langle, \rangle} \int_0^{2\pi/q} d\eta \int_0^{2\pi/q} d\xi \frac{2\mu - (\varepsilon_+ + \varepsilon_-)}{2(\varepsilon_+ - \varepsilon_-)^2} \text{Im} \langle u_+ | \frac{\partial \mathbf{H}}{\partial \eta} | u_- \rangle \langle u_- | \frac{\partial \mathbf{H}}{\partial \xi} | u_+ \rangle \quad (7)$$

where ε are the eigenvalues and u the corresponding eigenvectors of the matrix. The symbols $>$ and $<$ refer to the states above and below the gap. Our numerical results are based on this equation.

Our investigation of the magnetization in the gaps bears an interesting relationship to the work of [9], where the energy E per unit cell of the Hofstadter model was studied. E is the Legendre transform of Ω ,

$$E(\rho, \varphi) = \mu\rho - \Omega(\mu, \varphi), \quad (8)$$

and [9] focused especially on its minima for fixed ρ . The properties of the Legendre transform imply that maxima of Ω as a function of φ , i.e., points where $m = 0$ and $\sigma > 0$, are (local) minima of E . It follows from our semiclassical analysis (see below) that $E(\rho, \varphi)$ has a minimum in every gap for $\varphi = 1/q$ (see, for example, figure 2). It also follows from equation (8) that E has a cusp as a function of φ at the gaps, with tangent slopes given by the limiting values of m at the ends of the gap.

The Hofstadter model can be viewed as the result of Peierls substitution [13], which stipulates that in a weak magnetic field the classical Hamiltonian

$$H_B(\xi, \eta) = 2 \cos \xi + 2 \cos \eta \quad (9)$$

is quantized by imposing $[\xi, \eta] = 2\pi i \varphi$. Fluxes near $\varphi = 0$ can then be analysed by semiclassical methods where the role of \hbar is played by $2\pi\varphi$. The classical ξ - η phase space is the two dimensional torus. Since its area is $(2\pi)^2$, quantization of the torus is consistent provided that the number of states, $1/\varphi$, is an integer. For this reason we shall assume that $\varphi = 1/q$.

The classical Hamiltonian $H_B(\xi, \eta)$ is a Morse function with one minimum (at energy -4), one maximum (at energy 4) and two saddle points (at energy zero). It follows that the classical trajectories with $E \neq 0$ are contractible and bound a disc-like domain. Only the level set $E = 0$ winds around the torus.

Let

$$S(E) = \int_{H_B < E} d\xi \wedge d\eta \quad (10)$$

be the classical action associated with a trajectory of energy E . By the Bohr–Sommerfeld quantization rule, the negative part of the spectrum is given, to leading order in φ , by those energies E_n for which

$$S(E_n) = (n + \gamma)\varphi, \quad \gamma = 1/2, n = 1, \dots, \lfloor q/2 \rfloor. \quad (11)$$

This gives a good approximation to the spectrum, provided that φ is small and E is far from the separatrix. More precisely, one needs $\varphi \ll |E|$. The energy E_n of equation (11) is then an approximation to the n th energy band which is exponentially localized in energy near E_n . Near the separatrix one finds wider bands which we do not study [14]. We therefore assume below that $\mu \ll -\varphi$. The magnetization for $\mu \gg \varphi$ then follows by equation (2). The region which we do not study, $|\mu| = O(\varphi)$, becomes arbitrarily small in the limit $\varphi \rightarrow 0$. This is a limit we eventually take.

Fixing the chemical potential in the n th gap with $\mu < 0$, the semiclassical thermodynamic potential at $T = 0$ is

$$\Omega_b = \mu\rho - \sum_{j=0}^{n-1} E_j = \mu n\varphi - \varphi \sum_{j=0}^{n-1} S^{-1}((j + \gamma)\varphi). \quad (12)$$

By the second Euler–Maclaurin formula, the sum can be approximated by an integral (to $O(1/q^2)$),

$$\Omega_b(\mu, \varphi) = \mu n\varphi - \int_0^{\varphi n} S^{-1}(x) dx, \quad \mu < 0. \quad (13)$$

The magnetization in the n th gap is therefore

$$m_b = -\frac{1}{\Phi_0}(\mu - S^{-1}(n\varphi))n \quad (14)$$

and vanishes when $\mu = S^{-1}(n\varphi)$. Since $\gamma = 1/2$ this happens in the middle of the gap, a property also evident in figure 2.

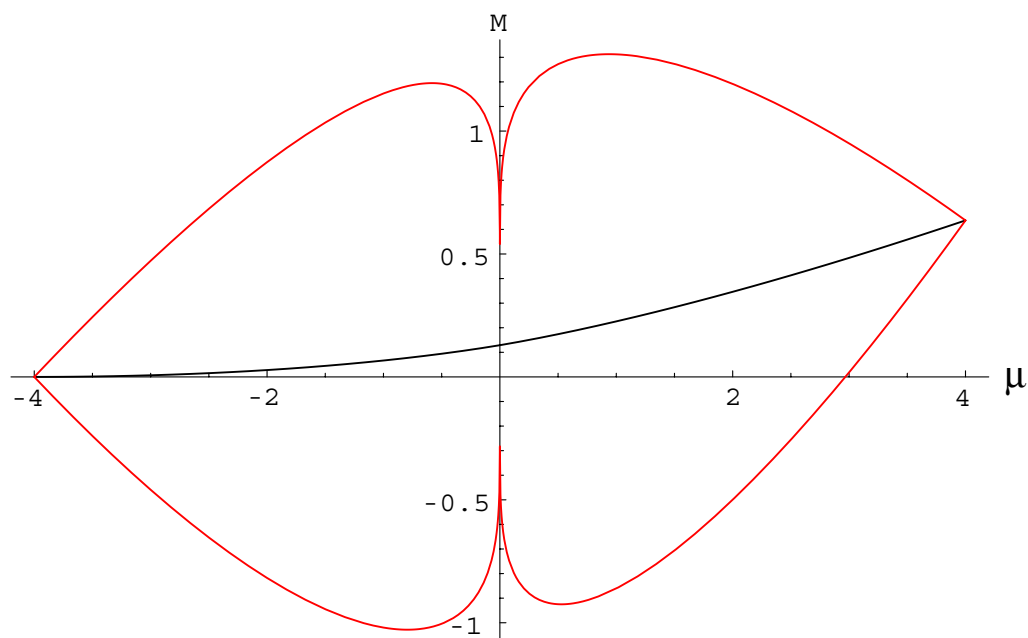


Figure 3. The central curve gives the limiting magnetization $m_l(\mu, \varphi = \infty)$ and the upper and lower curves form the lip $L_l(\mu, \varphi = 1)$.

Since the slope of m_b in the n th gap is n/Φ_0 , the magnetization increases in this interval from $-n(E_n - E_{n-1})/2\Phi_0$ to $+n(E_n - E_{n-1})/2\Phi_0$. The extremal value L_b of the magnetization in the n th gap is therefore

$$L_b = \pm \frac{n\varphi}{2\Phi_0} S^{-1'}(n\varphi). \quad (15)$$

Fixing the chemical potential μ and letting $\varphi \rightarrow 0$, the product $n\varphi$ approaches the limiting value $S(\mu)$, see (11). The envelope approaches

$$L_b(\mu, \varphi = 0) = \pm \frac{S(\mu)}{2\Phi_0 S'(\mu)}. \quad (16)$$

The graph of $L_b(\mu, 0)$ is shown in figure 2 overlaid with numerical results for the magnetization that follow from the (exact) equation (7). This graph is an analogue of the de Haas–van Alphen oscillations in metals [10].

$L_b(\mu, 0)$ is the mother of all lips; we shall argue below that the lips at other (rational) fluxes are deformations of it, in both the split Bloch and split Landau versions of the model. The lips associated with the split Landau level $L_l(\mu, 1/n)$, with integer n , are particularly simple deformations of the mother of all lips. This can be seen as follows: from equation (5)

$$L_l(\mu, 1/n) = \frac{1}{\Phi_0} \Omega_b(\mu, 0) - nL_b(\mu, 0). \quad (17)$$

Since Ω_b is a convex, and therefore continuous, function of μ , equation (17) describes a scaling of $L_b(\mu, 0)$ and a shifting of its baseline, see figure 3. The special case $m_l(\mu, \infty)$ ($n = 0$) is different; the lip is scaled to zero width and $m_l(\mu, \infty)$ is a continuous function of μ .

Although the actual shape of the lip $L_b(\mu, 0)$ cannot be expressed in terms of elementary functions, its qualitative features can be readily understood and are determined by the critical

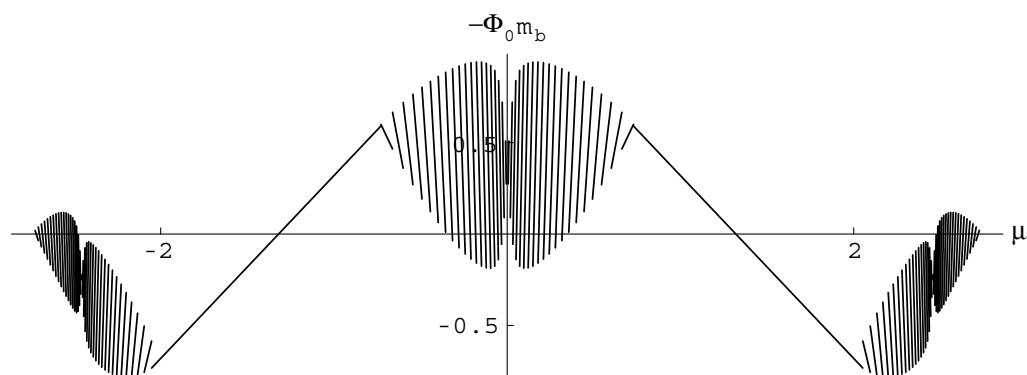


Figure 4. Plot of the magnetization as function of the chemical potential for flux that is $40/121$ of the unit of quantum flux through the unit cell of the tight binding Hofstadter model. The magnetization is plotted for values of chemical potential that correspond to a spectral gap.

points of the band function $H_B(\xi, \eta)$. Let $\delta\mu$ denote the distance of μ from a band edge. Since H_B is non-degenerate, the action $S(\mu)$ is linear in $\delta\mu$ near the maximum and the minimum—as for the harmonic oscillator. This says that the lip terminates linearly:

$$S(\mu) \sim |\delta\mu|, \quad L_b(\mu, 0) \sim \pm\delta\mu. \quad (18)$$

Near the separatrix at $E = 0$, which passes through the two saddle points of $H(\xi, \eta)$, the density of states diverges logarithmically and L_b vanishes logarithmically

$$S(\mu) - S(0) \sim \mu \log |\mu|, \quad L_b(\mu, 0) \sim \pm(\log \delta\mu)^{-1}. \quad (19)$$

Consider now the magnetization for φ close to a rational p/q . Since the gap edges are Hölder continuous of order $1/2$ in φ [15], the $q - 1$ gaps ($q - 2$ for even q) persist for nearby fluxes and so does the magnetization in these gaps. The q bands, however, splinter. This breakup can be described by semiclassical methods as follows [2]: for rational flux $\varphi = p/q$, the $q \times q$ matrix $\mathbf{H}(\varphi, \xi, \eta)$ gives rise to q magnetic Bloch bands $E_j(\xi, \eta)$, $j = 1, \dots, q$. Each magnetic Bloch band has one maximum, one minimum and two saddle points that have coinciding energies and are linked by a separatrix. This is a consequence of Chambers relation [16]. For φ close to p/q , the $q \times q$ matrix valued function is quantized by imposing the commutation relation $[\xi, \eta] = 2\pi i (\varphi - p/q)$.

The semiclassical strategy leading to the qualitative description of the lip at $\varphi = 0$ remains valid in this more general case, but the details are different. (For example, γ does not take a universal value $1/2$ but rather becomes a function of E and φ .) However, one still expects that the envelope of the magnetization is pinched linearly at the band edges and logarithmically at the separatrix. This gives all $L_b(\mu, p/q, j)$, $j = 1, \dots, q$, a lip-like shape, a distorted version of figure 2. Getting explicit expressions for $L_b(\mu, p/q, j)$ is a hard problem which lies beyond the scope of this paper. However, numerical support for our claims is given in figure 4. Here the magnetization as a function of the chemical potential is shown for the flux $\varphi = \frac{1}{3 + \frac{1}{40}}$ which is close to $1/3$. The three bands of $\varphi = 1/3$ split and give rise to rapidly oscillating magnetization with distorted lip-shaped envelopes.

Band splitting occurs on all energy scales of the Hofstadter butterfly, because of its fractal nature. We have shown that band splitting is always accompanied by de Haas–van Alphen

oscillations in the magnetization. The fractality of the spectrum is reflected by the fact that the magnetic oscillations occur on an arbitrarily small energy scale. The fingerprints of fractality are most evident for flux ratios φ which are irrational numbers that are well approximated by rationals (e.g. Liouville numbers). For such φ the graph of the magnetization as a function of μ , such as those shown in figures 2 and 4, is itself fractal, with magnetic oscillations bounded by lip-like envelopes appearing on infinitely many scales.

Acknowledgments

This work is supported by the Technion fund for promotion of research and by the EU grant HPRN-CT-2002-00277.

References

- [1] Harper P G 1955 *Proc. Phys. Soc. A* **68** 874–92
Hofstadter D 1976 *Phys. Rev. B* **14** 2239–49
- [2] Azbel M Ya 1964 *Sov. Phys.–JETP* **19** 634–45
Wilkinson M 1987 *J. Phys. A: Math. Gen.* **20** 4337–54
Wilkinson M 1984 *J. Phys. A: Math. Gen.* **17** 3459–76
Ramal R and Bellissard J 1990 *J. Physique* **51** 1803–30
Bellissard J, Kreft C and Seiler R 1991 *J. Phys. A: Math. Gen.* **24** 2329–53
Helffer B and Sjöstrand J 1990 *Mem. Soc. Math. France* **40** 1
- [3] Helffer B and Sjöstrand J 1989 *Mem. Soc. Math. France* **39** 1–139
Last Y 1994 *Commun. Math. Phys.* **164** 421–32
Gordon A, Jitomirskaya S, Last Y and Simon B 1997 *Acta Math.* **178** 169–83
- [4] Thouless D J, Kohmoto M, Nightingale M P and den Nijs M 1982 *Phys. Rev. Lett.* **49** 405–8
- [5] Osadchy D 2002 *MSc Thesis* Technion
Osadchy D and Avron J 2001 *J. Math. Phys.* **42** 5665–71
- [6] Wiegman P B and Zabrodin A V 1994 *Phys. Rev. Lett.* **72** 1890
- [7] Connes A 1990 *Geometrie Non Commutative* (Paris: InterEditions)
- [8] Albrecht C *et al* 2001 *Phys. Rev. Lett.* **86** 147
- [9] Hasegawa Y, Lederer P, Rice T M and Wiegmann P B 1989 *Phys. Rev. Lett.* **63** 907–10
Lieb E 1994 *Phys. Rev. Lett.* **73** 2158–61
- [10] Ashcroft N W and Mermin N D 1976 *Solid State Physics* (New York: Holt, Rinehart and Winston)
- [11] Streda P 1982 *J. Phys. C: Solid State Phys.* **15** L717–21
- [12] Bellissard J, van Elst A and Schultz-Baldes H 1994 *J. Math. Phys.* **35** 5373
Avron J E, Seiler R and Simon B 1994 *Commun. Math. Phys.* **159** 399–422
- [13] Peierls R 1933 *Z. Phys.* **3** 1055
Zak J 1968 *Phys. Rev.* **168** 686–95
Panati G, Spohn H and Teufel S 2002 *Preprint* math-ph/0212041
- [14] Thouless D J 1990 *Commun. Math. Phys.* **127** 187
Watson G I 1991 *J. Phys. A: Math. Gen.* **24** 4999–5010
Helffer B and Kerdelhué Ph 1995 *Commun. Math. Phys.* **173** 335
- [15] Avron J E, Van-Mouche P and Simon B 1990 *Commun. Math. Phys.* **132** 103–18
Avron J E, Van-Mouche P and Simon B 1991 *Commun. Math. Phys.* **139** 215 (erratum)
- [16] Chambers W 1965 *Phys. Rev. A* **140** 135–43